J Neuroimmune Pharmacol (2009) 4:338–349
DOI 10.1007/s11481-009-9153-7

ORIGINAL ARTICLE

Cannabinoid Regulation of Nitric Oxide Synthase I (nNOS) in Neuronal Cells

Skyla T. Carney · Michael L. Lloyd · Shanta E. MacKinnon · Doshandra C. Newton · Jenelle D. Jones · Allyn C. Howlett · Derek C. Norford

Received: 2 July 2008 / Accepted: 18 March 2009 / Published online: 14 April 2009

Abstract In our previous studies, CB_1 cannabinoid receptor agonists stimulated production of cyclic GMP and translocation of nitric oxide (NO)-sensitive guanylyl cyclase in neuronal cells (Jones et al., Neuropharmacology 54:23–30, 2008). The purpose of these studies was to elucidate the signal transduction of cannabinoid-mediated neuronal nitric oxide synthase (nNOS) activation in neuronal cells. Cannabinoid agonists CP55940 (2-[(1*S*,2*R*,5*S*)-5-hydroxy-2-(3-hydroxypropyl) cyclohexyl]-5-(2-methyloctan-2-yl) phenol), WIN55212-2 (*R*(+)-[2,3-dihydro-5-methyl-3-[(morpholinyl)methyl]pyrrolo[1,2,3-*de*]-1,4-benzoxazinyl]-(1-naphthalenyl)methanone mesylate), and the metabolically stable analog of anandamide, (*R*)-(+)-methanandamide stimulated NO production in N18TG2 cells over a 20-min period. Rimonabant (*N*-(piperidin-lyl)-5-(4-chlorophenyl)-1-(2,4-dichlorophenyl)-4-methyl-*H*-pyrazole-3-carboxamide), a CB_1 receptor antagonist, partially or completely curtailed cannabinoid-mediated NO production. Inhibition of NOS activity (N^G-nitro-L-arginine) or signaling via Gi/o protein (pertussis toxin) significantly limited NO production by cannabinoid agonists. Ca^{2+} mobilization was not detected in N18TG2 cells after cannabinoid treatment using Fluo-4 AM fluorescence. Cannabinoid-mediated NO production was attributed to nNOS activation since endothelial NOS and inducible NOS protein and mRNA were not detected in N18TG2 cells. Bands of 160 and 155 kDa were detected on Western blot analysis of cytosolic and membrane fractions of N18TG2 cells, using a nNOS antibody. Chronic treatment of N18TG2 cells with cannabinoid agonists downregulated nNOS protein and mRNA as detected using Western blot analysis and real-time polymerase chain reaction, respectively. Cannabinoid agonists stimulated NO production via signaling through CB_1 receptors, leading to activation of Gi/o protein and enhanced nNOS activity. The findings of these studies provide information related to cannabinoid-mediated NO signal transduction in neuronal cells, which has important implications in the ongoing elucidation of the endocannabinoid system in the nervous system.

Keywords CB_1 cannabinoid receptor · CP55940 · nitric oxide · gene expression · G-protein coupled receptors · G-proteins · neuronal nitric oxide synthase · methanandamide · 2-arachidonoylglycerol · real-time polymerase chain reaction · rimonabant (SR141716) · WIN55212-2

Howlett and Norford are guarantors of this work.

S. T. Carney · M. L. Lloyd · S. E. MacKinnon · D. C. Newton · D. C. Norford (✉)
Neuroscience of Drug Abuse Research Program,
Julius L. Chambers Biomedical/Biotechnology Research Institute,
North Carolina Central University,
700 George Street,
Durham, NC 27707, USA
e-mail: dnorford@nccu.edu

J. D. Jones · A. C. Howlett
Department of Physiology and Pharmacology,
Wake Forest University Health Sciences,
Winston-Salem, NC 27157, USA

Introduction

Nitric oxide (NO) is a highly reactive compound that can serve as a beneficial physiologic messenger or as a toxin in disease processes in various tissues (Schmidt and Walter 1994). NO is generated from L-arginine by oxidation–reduction reactions catalyzed by one of at least three isoforms of nitric oxide synthase (NOS), namely the neuronal (nNOS), endothelial (eNOS), and inducible (iNOS) isoforms (Alderton et al. 2001; Boucher et al. 1999; Knowles

and Moncada 1994). nNOS and eNOS are constitutive enzymes, whereas pro-inflammatory mediators induce the iNOS activity and gene expression. NO stimulates physiologic and pathophysiologic effects in neurons of the central and peripheral nervous systems (Christopherson and Bredt 1997). NO modulates neuronal function through release of neurotransmitters and regulation of excitability and firing in long-term depression, long-term potentiation, and memory processes of synaptic plasticity (Holscher 1997; Huang 1997; Ohkuma and Katsura 2001; Prast and Philippu 2001; Wang, et al. 2005). Elevation of NO production has also been associated with several neurological diseases such as Parkinson's disease, Alzheimer's disease, multiple sclerosis, and stroke (Duncan and Heales 2005). Many of the effects of excessive NO production have been described as detrimental. In contrast, it was shown that hyperphosphorylation, truncation, and aggregation of Tau protein were increased in an Alzheimer's disease model bred on an iNOS knockout mouse background (Colton et al. 2006), implicating a protective role for NO in the pathogenesis of this disease.

Endogenous and exogenous cannabinoids mediate their effects though activation of G-protein coupled receptors called CB_1 and CB_2 cannabinoid receptors (Palmer et al. 2002). CB_1 cannabinoid receptors have been found in brain and other nervous tissue, whereas CB_2 receptors have been detected mainly in immune cells and tissues (Howlett et al. 2002). CB_1 receptors and NOS have been closely associated in striatal (Fusco et al. 2004) and spinal cord (Salio et al. 2002) neurons. Activation of cannabinoid receptors by the endocannabinoid, anandamide, in the median eminence led to NO production, which could be curtailed by inhibition of NOS activity by L-*N*-arginine-methyl ester (L-NAME; Prevot et al. 1998). NO signaling has been shown to be involved in cannabinoid-mediated hypothermia and catalepsy (Azad et al. 2001). Furthermore, co-treatment of rats with L-NAME and WIN55212-2 enhanced hypothermia through a synergistic effect (Rawls et al. 2004). In chronic treatment experiments, repeated dosing of L-NAME inhibited the development of tolerance to the hypothermic and cataleptic effects of WIN55212-2 (Spina et al. 1998). Cannabinoids have been shown to protect against *N*-methyl-D-aspartate (NMDA) receptor-mediated neurotoxicity of retinal (El-Remessy et al. 2003) and cerebrocortical (Kim et al. 2006) neurons; these pathologic effects were believed to involve elevated NO production and generation of reactive nitrogen species (El-Remessy et al. 2003; Rameau et al. 2003; Rameau et al. 2007).

In our previous studies, cannabinoid agonists stimulated production of cyclic GMP and translocation of NO-sensitive guanylyl cyclase in neuronal cells (Jones et al. 2008). Signal transduction mechanisms and all subsequent downstream effects of cannabinoid-mediated NO production in neuronal cells have yet to be described. The purpose of these studies is to elucidate signal transduction mechanisms of the cannabinoid-mediated nNOS activation resulting in NO production in neuronal cells.

Materials and methods

Materials

The reagents were purchased from Sigma Chemical Company (St. Louis, MO, USA), unless otherwise stated. CP55940 (2-[(1*S*,2*R*,5*S*)-5-hydroxy-2-(3-hydroxypropyl) cyclohexyl]-5-(2-methyloctan-2-yl)phenol) and rimonabant (*N*-(piperidin-lyl)-5-(4-chlorophenyl)-1-(2,4-dichlorophenyl)-4-methyl-*H*-pyrazole-3-carboxamide) were provided by the National Institute on Drug Abuse drug supply program. WIN55212-2 (*R*(+)-[2,3-dihydro-5-methyl-3-[(morpholinyl) methyl]pyrrolo[1,2,3-*de*]-1,4-benzoxazinyl]-(1-naphthalenyl) methanone mesylate), (*R*)-(+)-methanandamide (MetAEA), and 2-arachidonoylglycerol were purchased from Tocris Cookson (Ellison, MO, USA). N^G-nitro-L-arginine (L-NNA) and N^G-nitro-D-arginine (D-NNA) were purchased from EMD Chemicals (Gibbstown, NJ, USA). NO indicator 4-amino-5-methylamino-2′,7′-difluorofluorescein diacetate, nuclear stain 4,6-diamidino-2-phenylindole dihydrochloride, Fluo-4 AM, and Prolong Antifade Mounting Media were purchased from Molecular Probes (Eugene, OR, USA). Components of Cytomix; human recombinant tumor necrosis factor-α (TNF-α; 1.1×10^5 units/mg protein); interleukin-1β (IL-1β; 2×0^5 units/mg); and interferon-γ (IFNγ; 2×10^4 units/mg) were purchased from R&D Systems (Minneapolis, MN, USA). Acrylamide, *N*,*N*,*N*′,*N*′-tetramethylethylene diamine, sodium dodecylsulfate (SDS), and polyvinylidine difluoride membranes were from BioRad Laboratories (Hercules, CA, USA). The nNOS rabbit polyclonal antibody (catalog no. 160870) was purchased from Cayman Chemical (Ann Arbor, MI, USA). Antibodies used to detect iNOS (mouse monoclonal IgG1 (catalog no. 610309)) and eNOS (mouse monoclonal IgG1 (catalog no. 610297)) were purchased from Transduction Laboratories (Lexington, KY, USA). Goat anti-rabbit IgG horseradish peroxidase (catalog no. G21234) and goat anti-mouse IgG horseradish peroxidase (catalog no. G21040) were purchased from Biosource International (Camarillo, CA, USA). Goat and mouse sera were from Gibco Life Technologies (Gaithersburg, MD, USA). Rainbow molecular markers and Enhanced Chemiluminescence Detection kit were from Amersham Biosciences (Piscataway, NJ, USA). The RNeasy Mini purification kit was from Qiagen (Valencia, CA, USA). The GeneAmp Gold RNA polymerase chain reaction (PCR) Core kit, TaqMan Universal PCR Master Mix, and Assays-on-Demand Gene Expression Assay mixes specific for mouse 18S ribosomal RNA, nNOS, iNOS,

and eNOS were from Applied Biosystems (Foster City, CA, USA). Primers for amplification of nNOS, iNOS, and eNOS were from Invitrogen (Carlsbad, CA, USA), and 18S ribosomal RNA primers were acquired from Amplicon (Pullman, WA, USA).

Cell culture

N18TG2 neuroblastoma cells (passage numbers 25–50) were maintained at 37°C under a 5% CO_2 atmosphere in Dulbecco's modified Eagle's medium/Ham's F-12 (1:1) with GlutaMax, sodium bicarbonate, and pyridoxine–HCl, supplemented with penicillin (100 units/ml) and streptomycin (100 μg/ml; Gibco Life Technologies) and 10% heat-inactivated bovine serum (JH Bioscience, Lenexa, KS, USA). An aliquot of drug stocks (stored at −20°C as 10 mM solutions in ethanol) or ethanol (control) was air-dried under sterile conditions in trimethylsilyl-coated glass test tubes and taken up in 100 volumes of 5 mg/ml fatty acid-free bovine serum albumin and serially diluted before being added (100 μl) to 75 cm^2 flasks containing 10 ml of media. Where indicated, N18TG2 cells were pretreated with the CB_1 antagonist rimonabant (1 μM) for 30 min prior to addition of agonists or at the times indicated before harvesting. Pertussis toxin (100 ng/ml final concentration; BIOMOL, Plymouth Meeting, PA, USA) was added to flasks containing fresh media 16 h before addition of agonists.

Measurement of NO production

NO production was measured using previously described methods (McCollum et al. 2007). Briefly, the cells were grown until 85% confluent on 12 mm uncoated glass cover slips in 24-well plates. The cells were loaded with 5 μM 4-amino-5-methylamino-2′,7′-difluorofluorescein (DAF-FM) diacetate (cell permeable form of DAF-FM) for 1 h in physiological saline solution (PSS; 150 mM NaCl, 5.4 mM KCl, 1.18 mM Na_2HPO_4, 1.17 mM $MgSO_4$, 6.0 mM $NaHCO_3$, 5.5 mM dextrose, 1 mM $CaCl_2$, 20 mM Na HEPES, pH 7.4). The cells were washed with PSS and treated for 20 min with cannabinoid agonists CP55940, WIN55212-2, or MetAEA in PSS. Intracellular DAF-FM diacetate is metabolized to DAF-FM, which combines with NO to produce a fluorescent benzotriazole derivative (Kojima et al. 1998) that when excited at 495 nm, emits light at 515 nm in direct proportion to the NO inside the cells. The cells were washed with phosphate-buffered saline (PBS; 138 mM NaCl, 5.4 mM KCl, 1.07 Na_2HPO_4, 1.1 mM KH_2PO_4, 15 mM Na HEPES, pH 7.4) and fixed with 0.5% glutaraldehyde in PBS at 4°C for 10 min, and nuclei were labeled with DAPI (Sugimoto et al. 2000; Takumida and Anniko 2001). Autofluorescence was minimized with 0.1% Na borohydride, which reduced spurious aldehyde combining with amines or proteins leading to background fluorescence (Clancy and Cauller 1998). The inverted cover slips were mounted onto glass slides using ProLong Antifade, and images from the slides were digitalized using identical exposure time and brightness settings for all conditions using a Nikon Eclipse E600 fluorescence microscope (Nikon Instruments, Melville, NY, USA). Quantitation of fluorescence was performed using Image Pro Plus 4.5 Software (Media Cybernetics, Bethesda, MD, USA). Ratios of green (NO-DAF-FM) to blue (DAPI) fluorescence were tabulated from three images of fields containing 15 or more cells, and the ratios were normalized to vehicle control=1 for each experiment (McCollum et al. 2007).

Reverse transcriptase-polymerase chain reaction

Following RNA isolation and quantitation, 1 μg of RNA from each sample was reverse-transcribed according to the manufacturer's specifications of the GeneAmp Gold RNA PCR Core kit. The resulting cDNA was amplified (35 cycles, AmpliTaqGold DNA polymerase and GeneAmp Gold kits) using primers described in previous studies to identify NOS isozymes (Dodd et al. 2000) and 18S ribosomal RNA as the loading control (28 cycles; Goidin et al. 2001). PCR products were detected from agarose gels (1.6%) after electrophoresis in TBE buffer containing 50 ng/ml ethidium bromide.

Real-time quantitative polymerase chain reaction (qPCR)

Total RNA was extracted from N18TG2 cells and purified using the Qiagen RNeasy Mini Kit, and purity was determined spectrophotometrically using the 260/280 ratio. Total RNA (1 μg) was reversed-transcribed into cDNA using random hexamers using the Applied Biosystems cDNA Archive Kit. Quantitative polymerase chain reaction (qPCR) reactions were performed using TaqMan Universal PCR Master Mix and Applied Biosystems gene expression assays (25 μl volumes) using an Applied Biosystems 7500 Real-time PCR System. Ribosomal 18S RNA was the reference standard gene, and relative quantitation was determined using the ΔΔCt method (Livak and Schmittgen 2001).

Western blot analysis

After treatment, N18TG2 cells were harvested with PBS-EDTA (2.7 mM KCl, 138 mM NaCl, 10.4 mM glucose, 1.5 mM KH_2PO_4, 8 mM Na_2HPO_4, 0.625 mM EDTA, pH 7.4). The cells were suspended in cold TME buffer (20 mM Tris–Cl, pH 7.4, 3 mM $MgCl_2$, 1 mM Na EDTA) with a protease inhibitor cocktail (set III, catalog no. 59134,

Calbiochem, La Jolla, CA, USA) having a broad ability to inhibit aspartic, cysteine, serine, and aminopeptidases. The cells were allowed to swell in the hypotonic solution (15 min) and then were homogenized with a glass–glass homogenizer and centrifuged at 1,000×*g* at 4°C for 10 min. The pellet (nuclear and cellular debris) was discarded, and the supernatant was centrifuged at 100,000×*g* for 30 min at 4°C. The membranes were resuspended in 1/20 the cytosol volume of 50 mM Tris–Cl buffer, pH 7.4, and aliquots of supernatant and membranes were stored at −80°C.

Rat forebrain cytosolic fractions were prepared from frozen whole rat brains purchased from Pel-Freeze (Rogers, AK, USA). The brains were thawed in ice-cold SME solution (320 mM sucrose, 5 mM $MgCl_2$, 2 mM Tris–EDTA). The brain tissue was homogenized in a glass–glass homogenizer in 2 ml of SME per gram of tissue and centrifuged at 1,000×*g* at 4°C for 10 min. The pellet was resuspended in 1 ml of SME for a second centrifugation, and the combined supernatants were centrifuged at 39,000×*g* at 4°C for 25 min. The cytosolic fractions were stored in aliquots at −80°C until use. The protein concentrations were determined using the Coomassie dye binding method (Bradford 1976).

Protein fractions were taken up in Laemmli's sample buffer with 1 mM dithiotheitol and heated at 60°C for 10 min, and equal amounts of protein (45 μg) were loaded per lane on SDS-6% polyacrylamide gels for electrophoresis (50 V for 30 min and then 120 V for 80 min). The proteins were transferred onto polyvinylidine difluoride membranes in Towbin's buffer (24 mM Tris Base, 192 mM glycine, 20% methanol, pH 8.3) for 1 h in the cold at 95 V using a Bio-Rad Trans-Blot Cell (BioRad Laboratories) with an ice pack. Blots were rinsed three times (5 min each) with Tris-buffered saline (TBS; 20 mM Tris–Cl, pH 7.4, 137 mM NaCl) and incubated with blocking solution (5% nonfat dry milk, 5% goat serum in TBS) at room temperature for 1 h. Blots were then incubated for 1 h at room temperature with an antibody (1:1,000) raised against a peptide comprising amino acids 1422–1433 of human nNOS (Bredt et al. 1991; Nakane et al. 1993) or amino acids 1418–1429 of mouse nNOS (Ogura et al. 1993). The blots were washed three times with TBS-T (TBS containing 0.1% Tween 20), incubated with horseradish peroxidase-coupled anti-rabbit IgG (1:8,000) for 1 h at room temperature, and washed five times with TBS-T followed by five times with NANOpure water. Immunoreactive bands were detected by enhanced chemiluminescence and exposure to Hyperfilm at various time intervals to obtain optimal signals. The blots were developed using a Kodak M35A X-OMAT processor (Rochester, NY, USA). Band densities were quantified using an Alpha Innotech Imager with AlphaEase software (Alpha Innotech, San Leandro, CA, USA). The average number of pixels per enclosed area after background correction was normalized to the control samples as 100%. The data were tested for statistically significant differences using one-way ANOVA and Dunnett's post hoc test or Student's *t* test (Prism version 4.00, GraphPad Software, San Diego, CA, USA).

Calcium imaging

N18TG2 cells were cultured on 25-mm glass cover slips in six-well plates for 48 h until 85% confluent. The cover slips were mounted in an Attofluor Cell Chamber (catalog no. A-7816, Molecular Probes). Cells were loaded with 5 μM Fluo-4 AM at room temperature, and the cover slips were washed three times with PSS before exposure to agonists. One milliliter of PSS was maintained in the chamber throughout the experimental period by removing 100 μl of PSS before each addition of 100 μl of cannabinoid agonists (0.3 nM–1 μM, final concentration). Serially increasing concentrations of agonists were added to the chamber every 60 s over a time course of 360 s. Intracellular Ca^{2+} measurements were taken from images containing up to 40 cells and captured at a rate of one frame per 983 ms, using a Zeiss LSM 510 Confocal microscope with LSM 510 software (Zeiss, Thornwood, NY, USA). Excitation and emitting wavelengths were 488 and 514 nm, respectively. The baseline was established as the fluorescence at the initial 30 s prior to adding drugs. For every experiment, the effects of cannabinoid agonists were compared to the dose-dependent response to bradykinin. The data were analyzed, and graphs were prepared using Prism 4.00.

Results

CB_1 agonists stimulate NO production in N18TG2 cells

N18TG2 neuroblastoma cells loaded with DAF-FM-diacetate were treated with cannabinoid receptor agonists CP55940, WIN55212-2, and the metabolically stable anandamide analog MetAEA (Fig. 1a). The low background fluorescence indicates that the cellular production of NO does not occur constitutively in these cells. Over the 20-min period of NO accumulation, all three cannabinoid receptor agonists produced maximal NO-DAF-FM fluorescence at 10 nM concentrations, indicating that the cells were extremely sensitive to agonist stimulation (Fig. 1b). Pretreatment with the CB_1 antagonist rimonabant reduced the NO-DAF-FM fluorescence in response to 10 nM CP55940 or WIN55212-2 and 1 μM MetAEA to the unstimulated control levels (Fig. 1c), indicating that the NO production could be attributed to CB_1 receptor stimulation. Previous studies had demonstrated that the CB_2 receptor is not expressed in N18TG2 cells (Jones et al. 2008), thereby

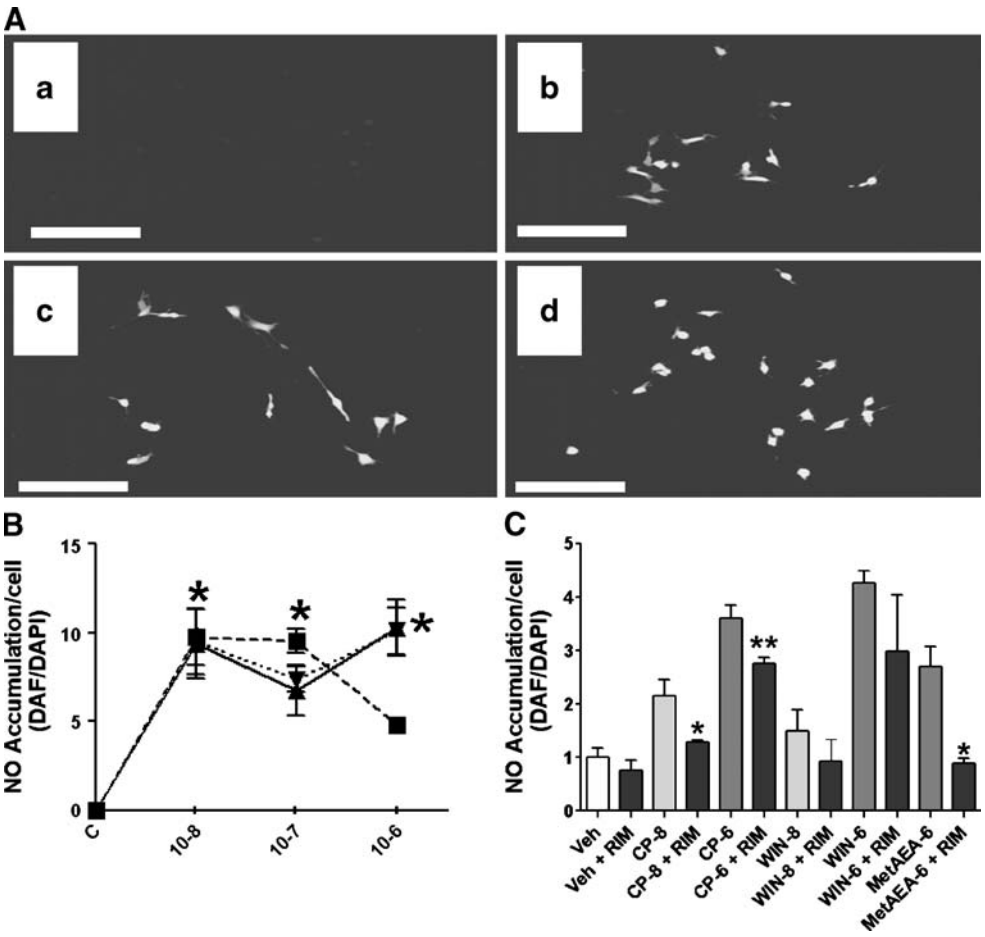

Fig. 1 Cannabinoids stimulate nitric oxide (*NO*) production in N18TG2 cells. **a** Cells were treated with vehicle (*a*), 1 μM CP55940 (*b*), WIN55212-2 (*c*), or methanandamide (*d*) for 20 min. NO production was detected from fluorescence of NO-DAF-FM (bar=100 μm). **b** Agonist log dose-response studies. N18TG2 cells were treated with the indicated concentrations of cannabinoid agonists (*squares* CP55940, *inverted triangles* WIN55212-2, *triangles* methanandamide). NO accumulation (20 min) in the cells was quantitated as the DAF-FM (*DAF*)/DAPI fluorescence intensity ratios mean± SEM from $N=3$ independent experiments. Statistically different from control (*C*; $*p<0.01$). **c** CB_1 antagonist on NO production by N18TG2 cells. Cells were pre-incubated (30 min) with 1 μM rimonabant (*RIM*) or vehicle (*Veh*) and subsequently treated (20 min) with Veh or 0.01 or 1 μM CP55940 (*CP*), WIN55212-2 (*WIN*), or methanandamide (*MetAEA*). Values are significantly different from agonist alone ($*p<0.01$, $**p<0.05$)

eliminating the possibility that these compounds might be acting on the CB_2 receptor. The observation that NO-DAF-FM fluorescence could not be reduced to background at 1 μM can be explained by the antagonist competition against a supra-maximal agonist concentration. Rimonabant did not independently impact the fluorescence of NO-DAF-FM, indicating that the CB_1 receptor does not exhibit constitutive activity to produce NO in these cells.

Mobilization of Ca^{2+} was determined in analysis of its role in cannabinoid-mediated NO production. Treatment of N18TG2 cells with endocannabinoid 2-arachidonoylglycerol and synthetic CB_1 receptor agonists CP55940 and WIN55212-2 did not mobilize Ca^{2+} in comparison to the effects of bradykinin (Fig. 2). These results suggest alternative signaling pathways for cannabinoid-mediated NO production other than through Ca^{2+} mobilization.

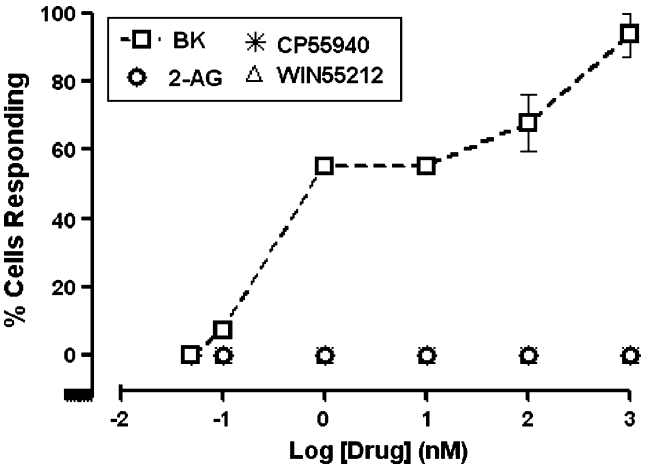

Fig. 2 Ca^{2+} mobilization in N18TG2 cells: cannabinoid agonists compared with bradykinin. N18TG2 cells loaded with 5 μM Fluo-4 AM were treated with 2-arachidonoylglycerol (*2-AG*), CP55940, WIN55212-2, or bradykinin (*BK*) at the indicated concentrations and fluorescence intensity evaluated using confocal microscopy. Data denote the percentage of total cells fluorescing above baseline over a 6-min experimental period and are presented as the mean±SEM from $N=5$–9 experiments

nNOS is responsible for the NO production

MetAEA-stimulated NO-DAF-FM fluorescence was attenuated by L-NNA, a non-selective NOS inhibitor, whereas the poorly active isomer D-NNA was not effective (Fig. 3). L-NNA similarly reduced NO-DAF-FM fluorescence

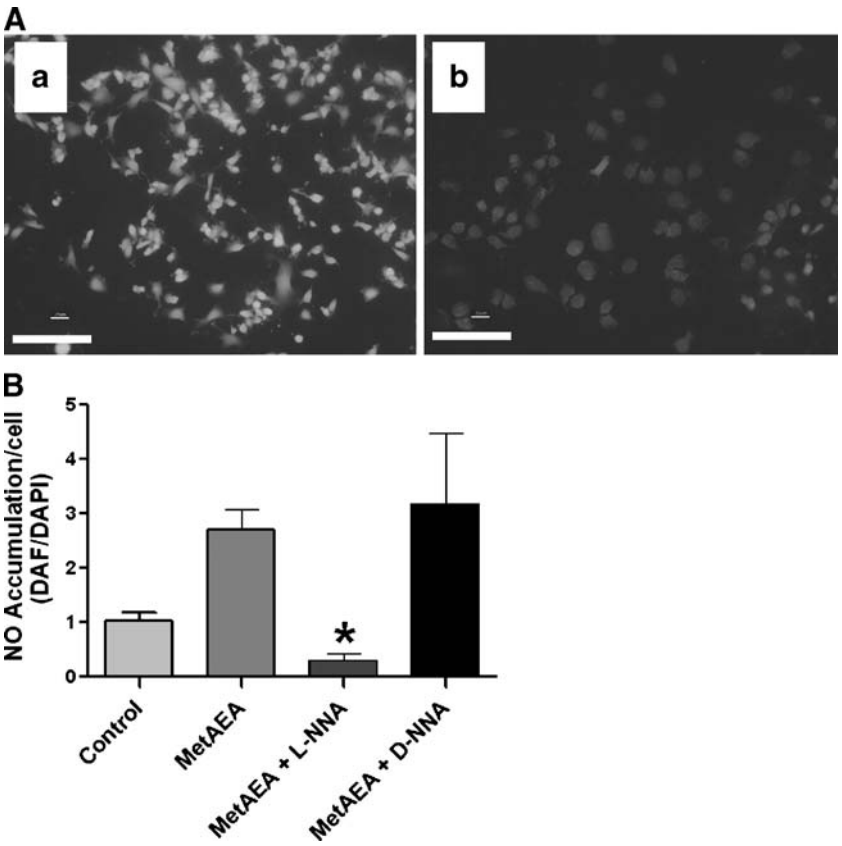

Fig. 3 Endocannabinoid-stimulated NO accumulation antagonized by a NOS inhibitor. **a** N18TG2 cells were treated with *a* methanandamide (MetAEA) alone (1 μM) or *b* following pretreatment with NOS inhibitor N^G-nitro-L-arginine (*L-NNA*; 1 μM; bar= 100 μm). **b** Quantitation of effects of NOS inhibitor L-NNA and its inactive enantiomer N^G-nitro-D-arginine (*D-NNA*; 1 μM) on methanandamide-stimulated NO accumulation in N18TG2 cells. Data are presented as the DAF/DAPI fluorescence intensity ratio (mean±SEM from N= 3 independent experiments). Values significantly different from those of MetAEA-stimulated cells (*p<0.01)

stimulated by CP55940 or WIN55212-2 (data not shown). Other inhibitors, including 1-amino-2-hydroxyguanidine *para*-toluenesulfonate, 7-nitroindazole, *S*-methylisothiourea sulfate, and L-thiocitrulline (a constitutive NOS inhibitor) also attenuated NO-DAF-FM fluorescence in response to CB_1 agonists (Carney and Norford, data not shown).

Because of the relatively poor selectivity exhibited by NOS inhibitors, the question of which NOS type was responsible for the NO production was addressed using protein and gene expression studies. As shown in Fig. 4a, antibodies staining for nNOS readily identified two bands on 6% polyacrylamide SDS-PAGE that are within the size range described previously by others (Grant et al. 2002; Putzke et al. 2000). Identical band patterns were detected in membrane-bound and 100,000×g cytosolic proteins from N18TG2 cells. The two bands may be representative of the expression of nNOS splice variants (Boissel et al. 1998; Wang et al. 1999) or post-translational modifications (Rameau et al. 2007). In contrast, there was no detectable eNOS found in the N18TG2 preparations on Western blots under conditions in which eNOS from human vascular endothelial cells could readily be observed (Fig. 4b). iNOS protein was not found in N18TG2 preparations, although iNOS could be detected among brain cytosolic proteins (Fig. 4c). In order to determine if an inflammatory stimulus could induce iNOS, cells were treated with TNF-α, IL-1β, and IFN-γ (10 ng/ml of each cytokine, Cytomix) for 8 to 20 h. In no experiment did we observe an induction of iNOS using conditions in which RAW 264.7 cells responded with a robust increase in iNOS protein (Norford et al. 1998).

In order to determine levels of gene expression of the three NOS isoforms, total RNA was isolated, and cDNA was amplified using previously published primers designed to detect expression of nNOS, eNOS, and iNOS genes (Dodd et al. 2000). Analysis by PCR indicated the expression of nNOS, but not eNOS or iNOS (Fig. 4d). cDNA prepared using the random primer method and quantified by qPCR also indicated that nNOS is expressed, whereas eNOS and iNOS were either undetectable or at the limits of detectability by this method (data not shown).

CB_1-stimulated NO production requires Gi/o proteins

CB_1 receptors activate Gi/o proteins, which have been implicated in the inhibition of adenylyl cyclase or stimulation of mitogen activated protein kinase phosphoryation (Mukhopadhyay et al. 2002). To test whether nNOS acti-

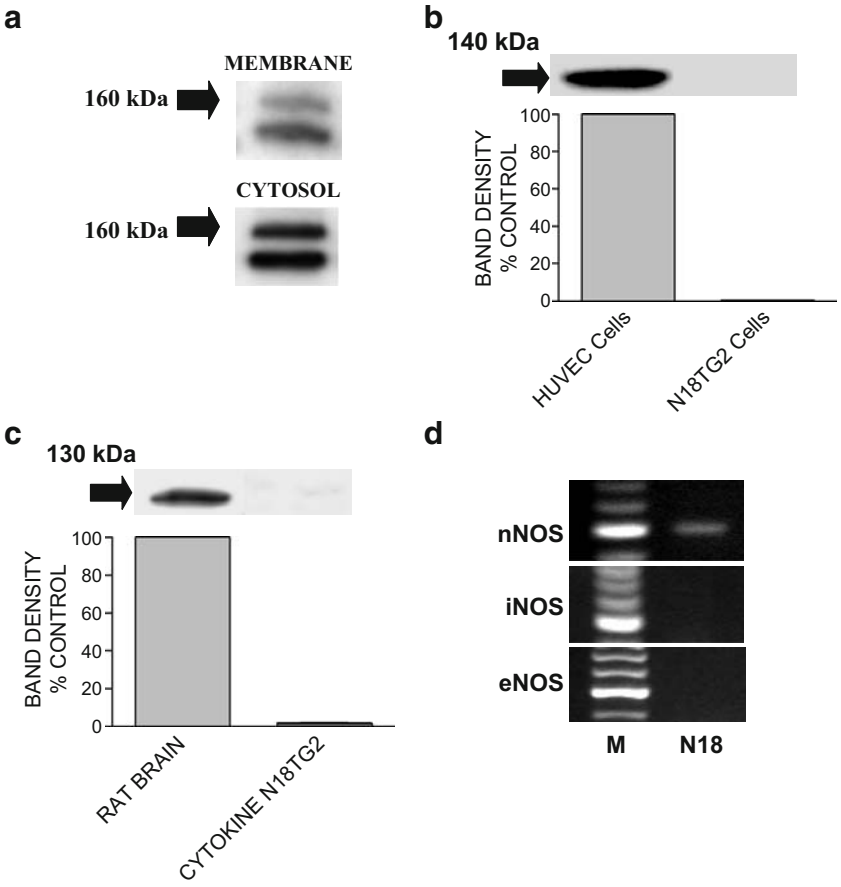

Fig. 4 NOS isozymes detected in N18TG2 cells. **a** Western blot analysis of nNOS in membrane and cytosolic fractions from N18TG2 cells is depicted. The 100,000×*g* cytosolic and the membrane fractions (45 μg) were subjected to SDS-PAGE (6% polyacrylamide) and stained with antisera (Cayman Chemicals) that recognizes nNOS protein. Blots are representative of at least three independent experiments. **b** Membrane fractions of human umbilical vein endothelial cells (HUVEC; 20 μg) and N18TG2 cells (45 μg) were separated by SDS-PAGE, and proteins were stained with an eNOS antibody. Band densitometry is normalized to eNOS levels in HUVEC cells as 100% (mean, *N*=3 experiments). **c** Cytosolic fractions of rat brain (7 μg) and Cytomix-treated N18TG2 cells (45 μg) were subjected to SDS-PAGE, and proteins were stained with an iNOS antibody. Band densitometry is normalized to iNOS in rat brain as 100% (mean, *N*=3 experiments). **d** Gel composite of PCR products denoting expression of nNOS, iNOS and eNOS genes by N18TG2 (N18) cells compared to a DNA marker (*M*). Western blot and PCR analyses of nNOS, iNOS, and eNOS protein and genes, respectively, are representative of three independent experiments

vation required Gi/o proteins, cells were pretreated with pertussis toxin, which ADP-ribosylates a cys residue on Gi/o family proteins that is critical for functional interaction with GPCRs. After Gi/o inactivation, CP55940, WIN55212-2, or MetAEA at >10-fold their maximal concentrations were not able to elicit stimulation above basal (Fig. 5), implicating Gi/o protein signaling as a requisite step to NO production.

Cellular levels of nNOS protein (both 160 and 155 kDa bands) were significantly decreased by treatment with prolonged incubation with WIN55212-2 (1 to 48 h), although the decline in response to CP55940 was not statistically significant (Figs. 6a and b). The decrement in nNOS protein was observed in both the cytosolic fraction as well as the membranes. nNOS mRNA was decreased at 8 and 24 h, with WIN55212-2 eliciting the most robust depletion of mRNA (Fig. 6c).

Discussion

The CB_1 receptor and nNOS protein have been identified in close proximity in brain areas suggestive of functional interactions that may be of importance in a variety of physiological states in which NO could serve either a paracrine or autocrine function. It has been shown that CB_1 receptor and nNOS are co-localized in neurons in lamina II and X regions of the spinal cord (Salio et al. 2002). In striatal medium spiny neurons, CB_1 receptors coexist on at least one third of the nNOS-expressing neurons (Azad et al. 2001; Fusco et al. 2004). In the hypothalamic preoptic area and arcuate nucleus, NOS and CB_1 receptors interact in thermoregulation (Rawls et al. 2004) and gonadotrophin-releasing hormone release (Prevot et al. 1998). In the hippocampus, the $\alpha_1\beta_1$ isoform of NO-sensitive guanylyl

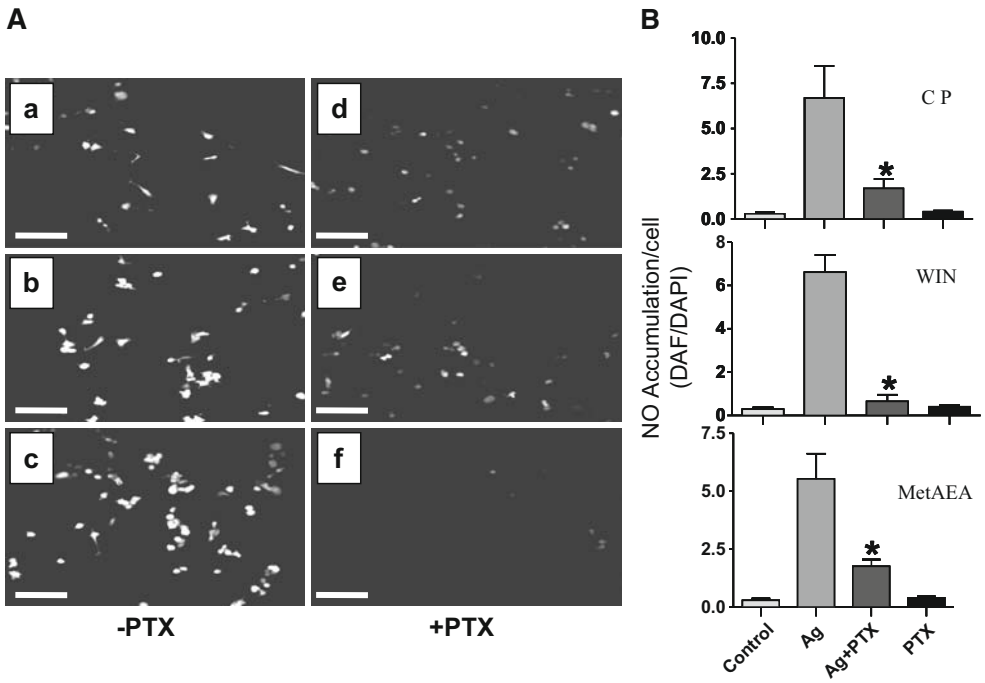

Fig. 5 The role of Gi/o protein on cannabinoid-mediated NO production in N18TG2 cells. **a** NO-DAF-FM fluorescence in N18TG2 cells treated (20 min) with 1 μM of CP55940 (CP) (*a*, *d*), WIN55212-2 (WIN) (*b*, *e*), or methanandamide (MetAEA) (*c*, *f*) in the absence (*a–c*) or presence (*d–f*) of pretreatment (16 h) with of pertussis toxin (*PTX*; 100 ng/ml; bar=100 μm). **b** Quantitation of NO accumulation stimulated by cannabinoid agonists (*Ag*) and modulated by PTX pretreatment is presented as the ratios of DAF/DAPI fluorescence intensity mean±SEM from $N=3$ independent experiments. Significantly different from agonist alone (*$p<0.01$)

cyclase was localized to the presynaptic CCK-positive (68%) GABAergic terminals (Szabadits et al. 2007), which has been co-expressed with the majority of the CB_1 receptors (Katona et al. 1999). Thus, NO originating from nNOS in cholinergic-stimulated pyramidal cells (Szabadits et al. 2007) could serve as a retrograde regulator of the NO-sensitive guanylyl cyclase in GABAergic interneurons (Makara et al. 2007), such that NO in combination with endocannabinoids could co-regulate depolarization-induced suppression of inhibition at these GABAergic synapses (Makara et al. 2007).

Similar to our observations of CB_1 receptor-stimulated NO production, Stefano's laboratory demonstrated that stimulation with anandamide led to NO production, which inhibited depolarization-evoked dopamine release in leech ganglia and stimulated neuropeptide release from the mammalian median eminence (Stefano et al. 1997; Prevot et al. 1998). Maccarrone and colleagues demonstrated that CB_1 receptor-stimulated NO production is involved in the anandamide translocation process (Maccarrone et al. 2006). These studies support the role of CB_1 receptor-stimulated NO production in various physiological processes.

In contrast, cannabinoid-stimulated NO production has not been universally observed in other neuronal preparations. In cultured rat cerebellar granule cells, depolarization-induced Ca^{2+} influx and subsequent NOS activation was reduced by WIN55212-2 via inhibition of voltage-gated Ca^{2+} channels (Hillard et al. 1999). In this preparation, the CB_1 antagonist rimonabant augmented depolarization-induced Ca^{2+} influx and NOS activation, suggestive of competitive inhibition of endocannabinoid (perhaps 2-arachidonoylglycerol)-mediated autocrine stimulation of nNOS (Hillard et al. 1999). This mechanism was very selective for voltage-gated Ca^{2+} channel-regulated NOS because the NMDA receptor-mediated Ca^{2+} influx and NOS activation were not inhibited (Hillard et al. 1999). Although the CB_1 receptor can regulate Ca^{2+} channels in the N18TG2 or its progenitor NG108-15 cells (Mackie et al. 1993; Sugiura et al. 1997b), this requires "differentiation" of the cells with cyclic AMP-generating agents, which was not done for our studies.

To investigate chronic effects of cannabinoids, Greenberg's laboratory evaluated the NO-DAF-FM fluorescence (20-min accumulation) in cultured mouse cortical neurons after 6 h treatment with NMDA (20 μM) in the presence or absence of WIN55212-2 (Kim et al. 2006). WIN55212-2 abrogated the excitotoxic NO accumulation, and either rimonabant treatment or the genetic knockout of the CB_1 receptor precluded the WIN55212-2 response. Activation of PKA by dibutyryl cAMP reversed the effects of WIN55212-2 (Kim et al. 2006), suggesting that prolonged reduction of PKA activity by the CB_1 agonist might lead to a net reduction of nNOS phosphorylation on a key serine residue phosphorylated in response to the NMDA stimulus. In our studies, cannabinoid agonists would be expected to promote a pattern of phosphorylation of nNOS that would be quite different from that of a neuron undergoing an excitotoxic reaction in response to NMDA (Rameau et al. 2004; Rameau et al. 2007). We determined that cannabinoid agonists stimulate a robust and prolonged translocation of NO-sensitive guanylyl cyclase from cytosol to the cell membranes (Jones et al. 2008). The $\alpha_1\beta_1$ isoform predominantly expressed in N18TG2 cells does not bind to the PDZ domains of

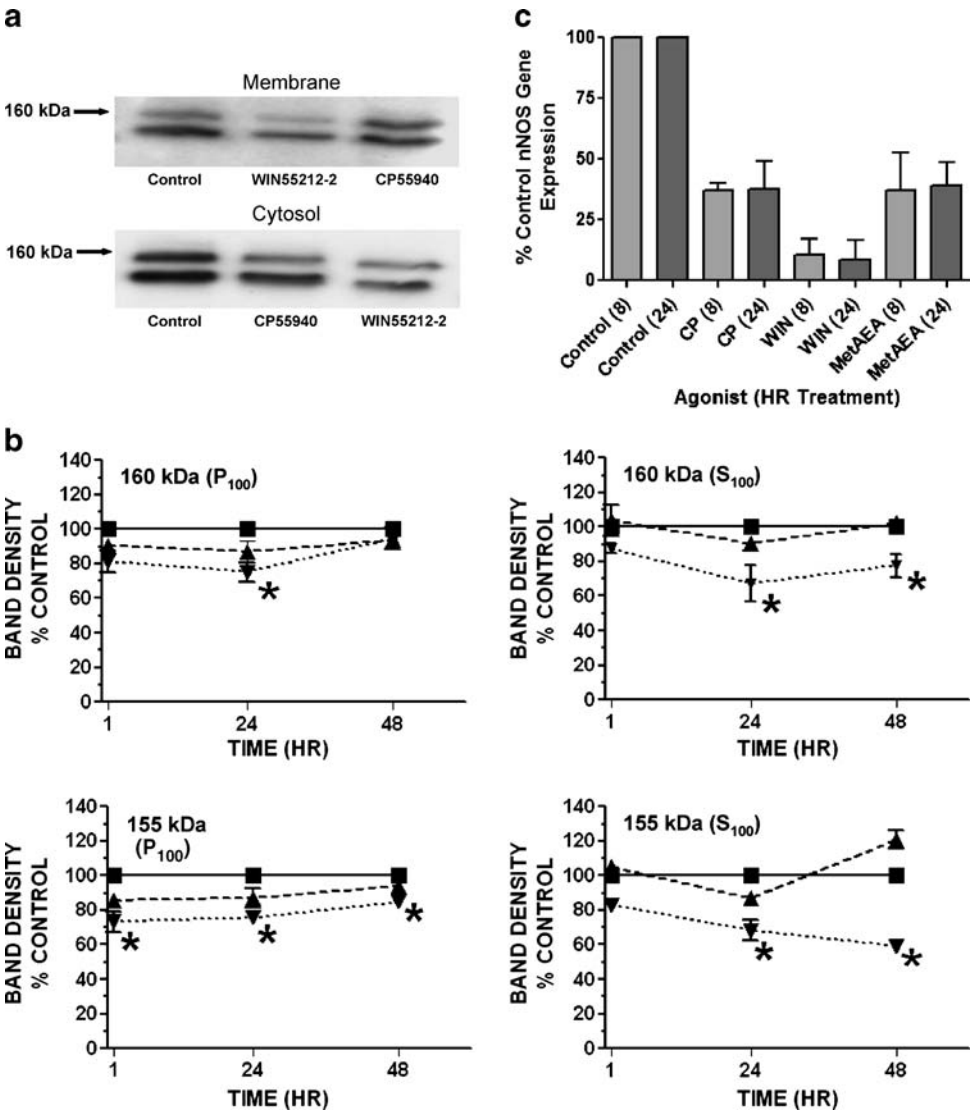

Fig. 6 The long-term regulation of nNOS protein and gene expression by cannabinoid agonists in N18TG2 cells. **a** Western blot analysis of membrane and cytosol fractions from N18TG2 cells treated with 1 μM CP55940 or WIN55212-2 for 24 h. **b** Densitometric analysis of the 160 and 155 kDa nNOS bands in membrane (P_{100}) and cytosolic (S_{100}) fractions (*squares*, control; *triangles*, CP55940; and *inverted triangles*,WIN55212-2). The data are presented as the mean±SEM (N=3 independent experiments). Values significantly different from vehicle-treated control (*p<0.01). **c** nNOS gene expression from N18TG2 cells treated for 8 or 24 h with vehicle (*Control*) or 1 μM of CP55940 (*CP*), WIN55212-2 (*WIN*), or methanandamide (*MetAEA*). RNA was reversed transcribed and quantified using qPCR analysis, and relative gene expression was compared with control samples using the ΔΔCt method. Data are the mean±SD from two identical experiments with samples run in triplicate for each qPCR trial

PSD95, suggesting that the NMDA receptor and Ca^{2+} influx is not the predominant regulator of this NO effector in the N18TG2 model.

The data obtained in our studies provide insights regarding cellular regulation of nNOS by CB_1 receptor stimulation. Western blots using 6% or 7.5% acrylamide gels routinely show two bands. This finding suggests that multiple nNOS isoforms are present in the N18TG2 cell. Post-translational phosphorylation of nNOS, which could incorporate as many as six to seven phosphates per monomer (Nakane et al. 1991), would result in multiple bands that could be discerned on SDS-PAGE. PKC, Ca^{2+}-calmodulin kinase II, PKA, and PKB (Akt) can regulate nNOS activity in cells and tissues (Bredt et al. 1992; Nakane et al. 1991; Rameau et al. 2007). Activation of nNOS by the excitotoxic stimulation of the NMDA receptor could be attributed to dephosphorylation of nNOS by calcineurin and PP1/PP2A (Rameau et al. 2003; Rameau et al. 2004). Thus, it is possible that the CB_1 receptor could stimulate NO production by a mechanism involving phosphorylation/dephosphorylation.

An alternative explanation for the observation of two nNOS bands on Western blots is the existence of splice variants. Other laboratories have reported isoforms such as the α and β forms described in mouse tissue (Brenman et al. 1996; Brenman et al. 1997; Putzke et al. 2000). An nNOSβ isoform lacking the 1.1 kB exon 2, which would result in a deletion of the PDZ domain, would be expected to be present in the cytosol but not in the membranes and would be expected to appear as a band of >30 kDa lower apparent MW on SDS-PAGE. Because the antibody that we used would have recognized both forms, our data for cytosol and membrane-associated nNOS do not support the existence of a splice variant exhibiting these properties.

A nNOS isoform in which exons 9 and 10 are deleted and therefore is missing the C-terminal portion of the dihydrofolate reductase domain is a lower molecular weight dysfunctional isoform that might serve a role in a cellular function

other than NO synthesis from L-arginine (Iwasaki et al. 1999; Ogura et al. 1993). The nNOSμ isoform, originally described in skeletal muscle and also found in brain (Ihara et al. 2006), possesses a 34-amino-acid insert that increases its apparent molecular weight. It should be noted that other alternative splicing of exons 1 and 2 can affect the untranslated region, leading to potentially altered regulation of mRNA stability and translation (Boissel et al. 2003; Brenman et al. 1997; Newton et al. 2003), but would not affect the mobility on Western blots. Studies with N18TG2 cells do not provide convincing evidence from conventional PCR analyses that would argue for the presence of alternative splice variants (Lloyd and Norford, unpublished observations).

A question remains regarding the source of Ca^{2+} that triggers NO production via nNOS in the N18TG2 model. Our studies indicate that potent CB_1 agonists fail to evoke a rise in intracellular Ca^{2+} within the first few minutes of activation. This finding contrasts with the findings of a PLC-mediated rapid rise in intracellular Ca^{2+} in neuroblastoma cells reported by Sugiura's laboratory (Sugiura et al. 1997a). In contrast, Sarne's laboratory demonstrated a slower increase in intracellular Ca^{2+} initiated by phosphorylation of a voltage-gated L channel (Rubovitch et al. 2002), which might coincide with the 20-min time course of NO accumulation in our studies. Alternatively, a Ca^{2+}-sensing receptor also triggers Ca^{2+} mobilization in these cells (Sesay et al. 2007). Other GPCRs such as the M2-muscarinic receptor also stimulate nNOS without an obvious Ca^{2+} transient (see discussion by Chistopoulos and El Fakahany 1999).

In summary, we have found an autocrine regulation of the CB_1 receptor-nNOS-NO-sensitive guanylyl cyclase in a model neuronal cell line. We demonstrated that, in contrast to the NMDA-mediated nNOS stimulation by calmodulin and modulated by Ca^{2+}-regulated kinases and phosphatase, NO appears to be produced in response to CB_1 receptor stimulation in a Gi/o-selective manner without an obvious Ca^{2+} transient. Continued stimulation of NO production results in reduction in mRNA and protein levels. Because nNOS can be found in both membrane and cytosolic fractions, it is possible that the CB_1-mediated nNOS activation might result entirely from kinases or phosphatases regulated by second messengers or by a Ca^{2+} transient occurring over a prolonged time or in response to an alternative stimulus. Our findings help to clarify the mechanism by which cannabinoids promote NO production in an autocrine or paracrine signaling in biological responses mediated by the CB_1 receptor.

Acknowledgments This work was supported by NIDA grants R01-DA03690, U24-DA12385, and K05-DA00182; NIGMS grants S06-GM008049 and R25-GM51757; and NCMHD grant P20-MD00175. These studies were in partial fulfillment of the M.S. degree in Biology at NCCU for STC, MLL, SEM, and DCN.

References

Alderton WK, Cooper CE, Knowles RG (2001) Nitric oxide synthases: structure, function and inhibition. Biochem J 357:593–615. doi:10.1042/0264-6021:3570593

Azad SC, Marsicano G, Eberlein I, Putzke J, Zieglgansberger W, Spanagel R, Lutz B (2001) Differential role of the nitric oxide pathway on Δ^9-THC-induced central nervous system effects in the mouse. Eur J Neurosci 13:561–568. doi:10.1046/j.1460-9568.2001.01431.x

Boissel JP, Schwarz PM, Forstermann U (1998) Neuronal-type NO synthase: transcript diversity and expressional regulation. Nitric Oxide 2:337–349. doi:10.1006/niox.1998.0189

Boissel JP, Zelenka M, Godtel-Armbrust U, Feuerstein TJ, Forstermann U (2003) Transcription of different exons 1 of the human neuronal nitric oxide synthase gene is dynamically regulated in a cell- and stimulus-specific manner. Biol Chem 384:351–362. doi:10.1515/BC.2003.041

Boucher JL, Moali C, Tenu JP (1999) Nitric oxide biosynthesis, nitric oxide synthase inhibitors and arginase competition for L-arginine utilization. Cell Mol Life Sci 55:1015–1028. doi:10.1007/s000180050352

Bradford MM (1976) A rapid and sensitive method for the quantitation of microgram quantities of protein utilizing the principle of protein-dye binding. Anal Biochem 72:248–254. doi:10.1016/0003-2697(76) 90527-3

Bredt DS, Hwang PM, Glatt CE, Lowenstein C, Reed RR, Snyder SH (1991) Cloned and expressed nitric oxide synthase structurally resembles cytochome P-450 reductase. Nature 351:714–718. doi:10.1038/351714a0

Bredt DS, Ferris CD, Snyder SH (1992) Nitric oxide synthase regulatory sites. Phosphorylation by cyclic AMP-dependent protein kinase, protein kinase C, and calcium/calmodulin protein kinase; identification of flavin and calmodulin binding sites. J Biol Chem 267:10976–10981

Brenman JE, Chao DS, Gee SH, McGee AW, Craven SE, Santillano DR, Wu Z, Huang F, Xia H, Peters MF, Froehner SC, Bredt DS (1996) Interaction of nitric oxide synthase with the postsynaptic density protein PSD-95 and alpha1-syntrophin mediated by PDZ domains. Cell 84:757–767. doi:10.1016/S0092-8674(00) 81053-3

Brenman JE, Xia H, Chao DS, Black SM, Bredt DS (1997) Regulation of neuronal nitric oxide synthase though alternative transcripts. Dev Neurosci 19:224–231. doi:10.1159/000111211

Christopherson KS, Bredt DS (1997) Nitric oxide in excitable tissues: physiological roles and disease. J Clin Invest 100:2424–2429. doi:10.1172/JCI119783

Chistopoulos A, El Fakahany EE (1999) The generation of nitric oxide by G protein-coupled receptors. Life Sci 64:1–15. doi:10.1016/S0024-3205(98) 00348-8

Clancy B, Cauller LJ (1998) Reduction of background autofluorescence in brain sections following immersion in sodium borohydride. J Neurosci Methods 83:97–102. doi:10.1016/S0165-0270(98) 00066-1

Colton CA, Vitek MP, Wink DA, Xu Q, Cantillana V, Previti ML, Van Nostrand WE, Weinberg B, Dawson H (2006) NO synthase 2 (*NOS2*) deletion promotes multiple pathologies in a mouse model of Alzheimer's disease. Proc Natl Acad Sci U S A 103:12867–12872. doi:10.1073/pnas.0601075103

Dodd F, Limoges M, Boudreau RTM, Rowden G, Murphy PR, Too CKL (2000) L-Arginine inhibits apoptosis via a NO-dependent mechanism in Nb2 Lymphoma cells. J Cell Biochem 77:624–634. doi:10.1002/(SICI) 1097-4644(20000615) 77:4<624::AID-JCB10>3.0.CO;2-M

Duncan AJ, Heales SJ (2005) Nitric oxide and neurological disorders. Mol Aspects Med 26:67–96. doi:10.1016/j.mam.2004.09.004

El-Remessy AB, Khalil IE, Matrogoon S, Abou-Mohamed G, Tsai N, Roon P, Caldwell RB, Caldwell RW, Green K, Liou GI (2003) Neuroprotective effect of (-) Δ^9-tetrahydrocannabinol and cannabidiol in N-methyl-D-aspartate-induced retinal neurotoxicity. Am J Pathol 163:1997–2008

Fusco FR, Martorana A, Giampa C, De March Z, Farini D, D'Angelo V, Sancesario G, Bernardi G (2004) Immunolocalization of CB1 receptor in rat striatal neurons: a confocal microscopy study. Synapse 53:159–167. doi:10.1002/syn.20047

Goidin D, Mamessier A, Staquet MJ, Schmitt D, Berthier-Vergnes O (2001) Ribosomal 18S RNA prevails over glyceraldehyde-3-phosphate dehydrogenase and beta actin genes as internal standard for quantative comparison of mRNA levels in invasive and noninvasive human melanoma cell subpopulation. Anal Biochem 295:17–21. doi:10.1006/abio.2001.5171

Grant MK, Cuadra AE, El-Fakahany EE (2002) Endogenous expression of nNOS protein in several neuronal cell lines. Life Sci 71:813–817. doi:10.1016/S0024-3205(02) 01732-0

Hillard CJ, Muthian S, Kearn CS (1999) Effects of CB(1) cannabinoid receptor activation on cerebellar granule cell nitric oxide synthase activity. FEBS Lett 459:277–281. doi:10.1016/S0014-5793(99) 01253-3

Holscher C (1997) Nitric oxide, the enigmatic neuronal messenger: its role in synaptic plasticity. Trends Neurosci 20:298–303. doi:10.1016/S0166-2236(97) 01065-5

Howlett AC, Barth F, Bonner TI, Cabral G, Casellas P, Devane WA, Felder CC, Herkenham M, Mackie K, Martin BR, Mechoulam R, Pertwee RG (2002) International Union of Pharmacology. XXVII. Classification of cannabinoid receptors. Pharmacol Rev 54:161–202. doi:10.1124/pr.54.2.161

Huang EP (1997) Synaptic plasticity: a role for nitric oxide in LTP. Curr Biol 7:R141–R143. doi:10.1016/S0960-9822(97) 70073-3

Ihara H, Kuwamura M, Atsuta M, Nihonmatsu I, Okada T, Mukamoto M, Kozaki M (2006) Expression of neuronal nitric oxide synthase variant, nNOS-μ, in rat brain. Nitric Oxide 15:13–19. doi:10.1016/j.niox.2005.11.011

Iwasaki T, Hori H, Hayashi Y, Nishino T, Tamura K, Oue S, Iizuka T, Ogura T, Esumi H (1999) Characterization of mouse nNOS2, a natural variant of neuronal nitric-oxide synthase produced in the central nervous system by selective alternative splicing. J Biol Chem 274:17559–17566. doi:10.1074/jbc.274.25.17559

Jones JD, Carney ST, Vrana KE, Norford DC, Howlett AC (2008) Cannabinoid receptor-mediated translocation of NO-sensitive guanylyl cyclase and production of cyclic GMP in neuronal cells. Neuropharmacology 54:23–30. doi:10.1016/j.neuropharm.2007.06.027

Katona I, Sperlagh B, Sik A, Kafalvi A, Vizi ES, Mackie K, Freund TF (1999) Presynaptically located CB1 cannabinoid receptors regulate GABA release from axon terminals of specific hippocampal interneurons. J Neurosci 19:4544–4558

Kim SH, Won SJ, Mao XO, Jin K, Greenberg DA (2006) Molecular mechanisms of cannabinoid protection from neuronal excitotoxicity. Mol Pharmacol 69:691–696

Knowles RG, Moncada S (1994) Nitric oxide synthases in mammals. Biochem J 298:249–258

Kojima H, Nakatsubo N, Kikuchi K, Kawahara S, Kirino Y, Nagoshi H, Hirata Y, Nagano T (1998) Detection and imaging of nitric oxide with novel fluorescent indicators: diaminofluoresceins. Anal Chem 70:2446–2453. doi:10.1021/ac9801723

Livak KJ, Schmittgen TD (2001) Analysis of relative gene expression data using real-time quantitative PCR and the 2(−ΔΔ Ct). Methods Methods 25:402–408

Maccarrone M, Fiori A, Bari M, Granata F, Gasperi V, De Stefano ME, Finazzi-Agro A, Strom R (2006) Regulation by cannabinoid receptors of anandamide transport across the blood-brain barrier and through other endothelial cells. Thromb Haemost 95:117–127

Mackie K, Devane WA, Hille B (1993) Anandamide, an endogenous cannabinoid, inhibits calcium currents as a partial agonist in N18 neuroblastoma cells. Mol Pharmacol 44:498–503

Makara JK, Katona I, Nyiri G, Nemeth B, Ledent C, Watanabe M, de Vente J, Freund TF, Hajos N (2007) Involvement of nitric oxide in depolarization-induced suppression of inhibition in hippocampal pyramidal cells during activation of cholinergic receptors. J Neurosci 27:10211–10222. doi:10.1523/JNEUROSCI.2104-07.2007

McCollum L, Howlett AC, Mukhopadhay S (2007) Anandamide-mediated CB_1/CB_2 cannabinoid receptor-independent nitric oxide production in rabbit aortic endothelial cells. J Pharmacol Exp Ther 321:930–937. doi:10.1124/jpet.106.117549

Mukhopadhyay S, Shim JY, Assi AA, Norford D, Howlett AC (2002) CB(1) cannabinoid receptor-G protein association: a possible mechanism for differential signaling. Chem Phys Lipids 121:91–109. doi:10.1016/S0009-3084(02) 00153-6

Nakane M, Mitchell J, Forstermann U, Murad F (1991) Phosphorylation by calcium calmodulin-dependent protein kinase II and protein kinase C modulates the activity of nitric oxide synthase. Biochem Biophys Res Commun 180:1396–1402. doi:10.1016/S0006-291X(05) 81351-8

Nakane M, Schmidt HH, Pollock JS, Forstermann U, Murad F (1993) Cloned human brain nitric oxide synthase is highly expressed in skeletal muscle. FEBS Lett 316:175–180. doi:10.1016/0014-5793(93) 81210-Q

Newton DC, Bevan SC, Choi S, Robb GB, Millar A, Wang Y, Marsden PA (2003) Translational regulation of human neuronal nitric-oxide synthase by an alternatively spliced 5′-untranslated region leader exon. J Biol Chem 278:636–644. doi:10.1074/jbc.M209988200

Norford DC, Koo JS, Gray T, Alder K, Nettesheim P (1998) Expression of nitric oxide synthase isoforms in normal human tracheobronchial epithelial cells in vitro: dependence on retinoic acid and the state of differentiation. Exp Lung Res 24:355–366

Ogura T, Yokoyama T, Fujisawa H, Kurashima Y, Esumi H (1993) Structural diversity of neuronal nitric oxide synthase mRNA in the nervous system. Biochem Biophys Res Commun 193:1014–1022. doi:10.1006/bbrc.1993.1726

Ohkuma S, Katsura M (2001) Nitric oxide and peroxynitrite as factors to stimulate neurotransmitter release in the CNS. Prog Neurobiol 64:97–108. doi:10.1016/S0301-0082(00) 00041-1

Palmer SL, Thakur GA, Makriyannis A (2002) Cannabinergic ligands. Chem Phys Lipids 12:3–19. doi:10.1016/S0009-3084(02) 00143-3

Prast H, Philippu A (2001) Nitric oxide as a modulator or neuronal function. Prog Neurobiol 64:51–68. doi:10.1016/S0301-0082(00) 00044-7

Prevot V, Rialas CM, Croix D, Salzet M, Dupouy JP, Poulain P, Beauvillain JC, Stefano GB (1998) Morphine and anandamide coupling to nitric oxide stimulates GnRH and CRF release from rat median eminence: neurovascular regulation. Brain Res 790:236–244. doi:10.1016/S0006-8993(98) 00066-3

Putzke J, Seidel B, Huang PL, Wolf G (2000) Differential expression of alternatively spliced isoforms of neuronal nitric oxide synthase (nNOS) and N-methyl-D-aspartate receptors (NMDAR) in knockout mice deficient in nNOS alpha (nNOS alpha(Delta/Delta) mice). Brain Res Mol Brain Res 85:13–23. doi:10.1016/S0169-328X(00) 00220-5

Rameau GA, Chiu LY, Ziff EB (2003) NMDA receptor regulation of nNOS phosphorylation and induction of neuron death. Neurobiol Aging 24:1123–1133. doi:10.1016/j.neurobiolaging.2003.07.002

Rameau GA, Chiu LY, Ziff EB (2004) Bidirectional regulation of neuronal nitric-oxide synthase phosphorylation at serine 847 by the N-methyl-D-aspartate receptor. J Biol Chem 279:14307–14314. doi:10.1074/jbc.M311103200

Rameau GA, Tukey DS, Garcin-Hosfield ED, Titcombe RF, Misra C, Khatri L, Getzoff ED, Ziff EB (2007) Biphasic coupling of neuronal nitric oxide synthase phosphorylation to the NMDA receptor regulates AMPA receptor trafficking and neuronal cell death. J Neurosci 27:3445–3455. doi:10.1523/JNEUROSCI.4799-06.2007

Rawls SM, Tallarida RJ, Gray AM, Geller EB, Adler MW (2004) L-NAME (N omega-nitro-L-arginine methyl ester), a nitric-oxide synthase inhibitor, and WIN 55212–2 [4, 5-dihydro-2-methyl-4 (4-morpholinylmethyl)-1-(1-naphthalenyl-carbonyl)-6 H-pyrrolo [3, 2, 1ij]quinolin-6-one], a cannabinoid agonist, interact to evoke synergistic hypothermia. J Pharmacol Exp Ther 308:780–786. doi:10.1124/jpet.103.054668

Rubovitch V, Gafni M, Sarne Y (2002) The cannabinoid agonist DALN positively modulates L-type voltage-dependent calcium-channels in N18TG2 neuroblastoma cells. Brain Res Mol Brain Res 101:93–102. doi:10.1016/S0169-328X(02) 00174-2

Salio C, Fischer J, Franzoni MF, Conrath M (2002) Pre- and postsynaptic localizations of the CB1 cannabinoid receptor in the dorsal horn of the rat spinal cord. Neuroscience 110:755–764. doi:10.1016/S0306-4522(01) 00584-X

Schmidt HH, Walter U (1994) NO at work. Cell 78:919–925. doi:10.1016/0092-8674(94) 90267-4

Sesay J, Somasundaram C, Howlett AC, Diz DI, Awumey EM (2007) Ca^{2+}-sensing receptor signaling in mouse neuroblastoma cells: A model for the perivascular sensory nerve Ca^{2+}-sensing receptor. Hypertension 50:e124

Spina E, Trovati A, Parolaro D, Giagnoni G (1998) A role of nitric oxide in WIN 55,212–2 tolerance in mice. Eur J Pharmacol 343:157–163. doi:10.1016/S0014-2999(97) 01543-4

Stefano GB, Salzet B, Rialas CM, Pope M, Kustka A, Neenan K, Pryor S, Salzet M (1997) Morphine- and anandamide-stimulated nitric oxide production inhibits presynaptic dopamine release. Brain Res 763:63–68. doi:10.1016/S0006-8993(97) 00403-4

Sugimoto K, Fujii S, Takemasa T, Yamashita K (2000) Detection of intracellular nitric oxide using a combination of aldehyde fixatives with 4, 5-diaminofluorescein diacetate. Histochem Cell Biol 113:341–347

Sugiura T, Kodaka T, Kondo S, Nakane S, Kondo H, Waku K, Ishima Y, Watanabe K, Yamamoto I (1997a) Is the cannabinoid CB1 receptor a 2-arachidonoylglycerol receptor? Structural requirements for triggering a Ca2+transient in NG108–15 cells. J Biochem 122:890–895

Sugiura T, Kodaka T, Kondo S, Tonegawa T, Nakane S, Kishimoto S, Yamashita A, Waku K (1997b) Inhibition by 2-arachidonoylglycerol, a novel type of possible neuromodulator, of the depolarization-induced increase in intracellular free calcium in neuroblastoma x glioma hybrid NG108–15 cells. Biochem Biophys Res Commun 233:207–210. doi:10.1006/bbrc.1997.6425

Szabadits E, Cserep C, Ludanyi A, Katona I, Gracia-Llanes J, Freund TF, Nyiri G (2007) Hippocampal GABAergic synapses possess the molecular machinery for retrograde nitric oxide signaling. J Neurosci 27:8101–8111. doi:10.1523/JNEUROSCI.1912-07.2007

Takumida M, Anniko M (2001) Detection of nitric oxide in the guinea pig inner ear, using a combination of aldehyde fixative and 4, 5-diaminofluorescein diacetate. Acta Otolaryngol 121:460–464. doi:10.1080/000164801300366589

Wang Y, Newton DC, Marsden PA (1999) Neuronal NOS: gene structure, mRNA diversity, and functional relevance. Crit Rev Neurobiol 13:21–43

Wang HG, Lu F, Jin I, Udo H, Kandel ER, de Vente J, Walter U, Lohamann SM, Hawkins RD, Antonova I (2005) Presynaptic and postsynaptic roles of NO, cGK, and RhoA in long-lasting potentiation and aggregation of synaptic proteins. Neuron 45:389–403. doi:10.1016/j.neuron.2005.01.011